NEAR FIELD SMALL EARTHQUAKE -- COMPUTER SIMULATION

J. Theodore Cherry

Systems, Science and Software

Prepared for:

Air Force Office of Scientific Research
Advanced Research Projects Agency

31 October 1974

SYSTEMS, SCIENCE AND SOFTWARE

SSS-R-75-2475
Draft

NEAR FIELD SMALL EARTHQUAKE--COMPUTER SIMULATION

Final Report

Project Manager: J. Theodore Cherry (714) 453-0060

Sponsored by
Air Force Office of Scientific Research
Arlington, Virginia 22209
ARPA Order No. 2134

Program Code 2F10
Contract No. F44620-72-C-0051
Effective Date of Contract: 1 June 1972
Contract Completion Date: 30 June 1974

S³ Project 195

October 31, 1974

P.O BOX 1620, LA JOLLA, CALIFORNIA 92037, TELEPHONE (714) 453-0060

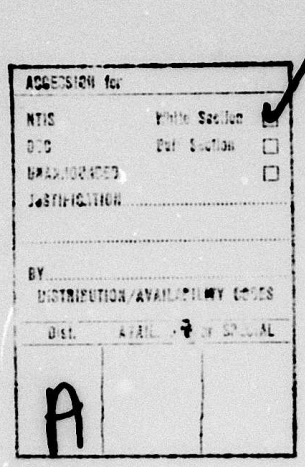

INTRODUCTION

A three dimensional (3D) finite difference code is being developed which will perform a deterministic simulation of a stick slip earthquake. The primary goal of this research effort is to obtain an earthquake's equivalent elastic source in a form which is suitable for propagation to teleseismic distances. Normalization of the earthquake model to the near field data obtained at Bear Valley is expected to furnish the required validation of the model.

RESULTS

In order to obtain a 3D code that is both computationally efficient and still flexible enough to permit nonlinear material response in the fault zone, a technique was developed which links a special purpose small deformation linear elastic code to a nonlinear material response code.

This link was tested in two dimensions by merging CRAM,[2] which contains the two dimensional fault model reported by Cherry,[1] and a special purpose linear code which assumes a Hooke's Law Material behavior. The difference equation used in CRAM to simulate the fault surface and the assumed nonlinear material behavior in the fault zone are given in Appendices A, B and C. The difference equations for the 2D linear code are given in Appendix D.

Calculation 5A was used as the test problem. This calculation[1] featured a 5 km fault, a rupture velocity of 2.15 km/sec and a dynamic stress drop of 0.5 kbar. A schematic of the calculation is shown in Fig. 1. This calculation was rerun using the linear code linked to CRAM. The CRAM grid was a rectangle with dimensions 13 km × 7 km, sufficient to cover the fault and the nonlinear region in the fault zone. Calculations outside this rectangular region were performed by the linear code.

Comparison between the original calculation 5A and the new calculation in which the linear code was linked to CRAM

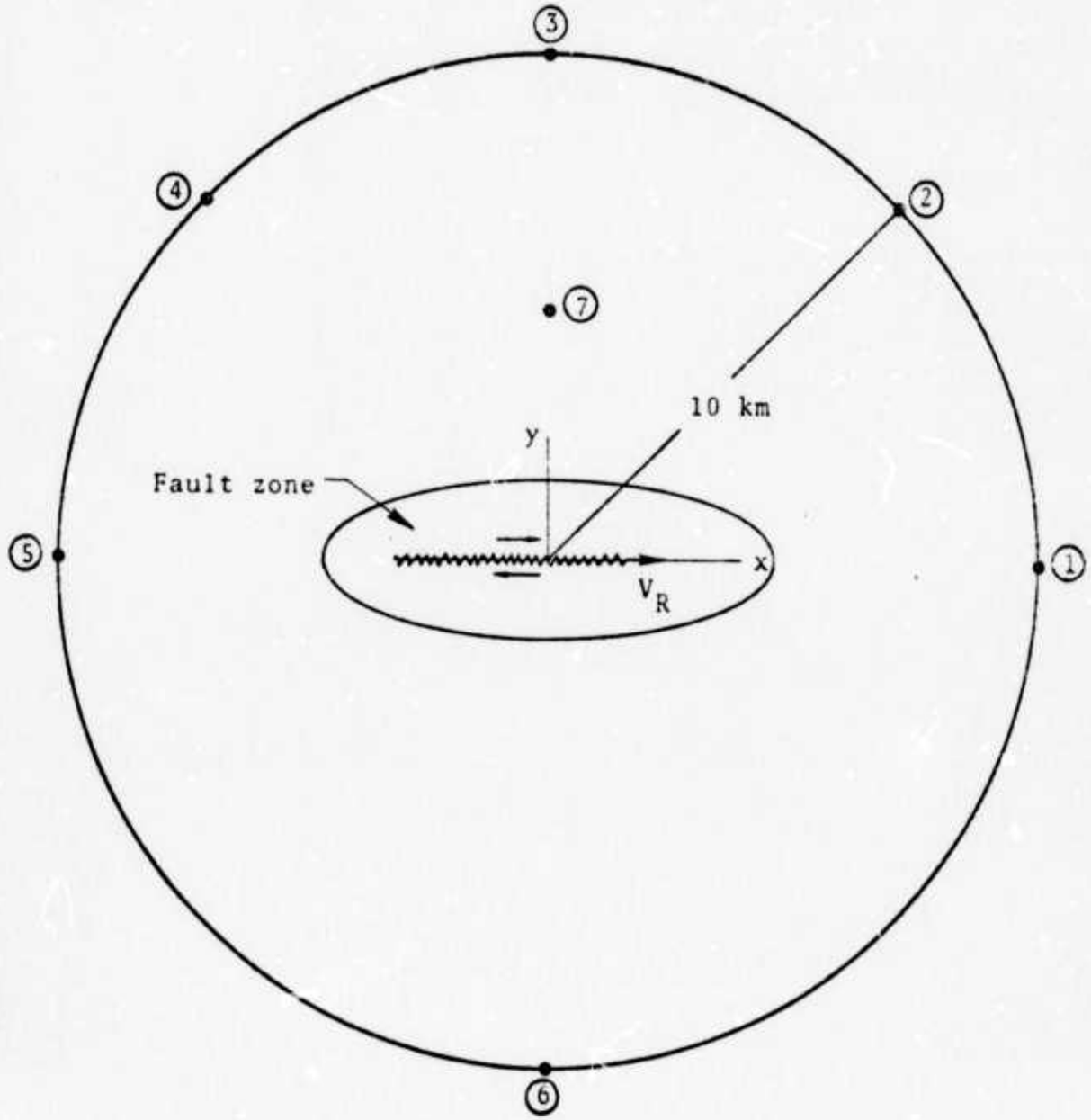

Figure 1. Stations monitored during calculation. The origin of the x-y coordinate system is in the center of the fault.

is given in Figs. 2 through 11. Agreement between the two calculations is excellent.

The motivation for using the linear code for calculations in the small displacement elastic regime is to reduce both computation time and computer costs. The new calculation, using the link, reduced the cost of the simulation by a factor of 4.3.

A three dimensional (3D) linear elastic code was developed (Appendix E) and the framework for linking to a 3D nonlinear code, containing the stick-slip fault model, was included in the linear code.

In order to debug the 3D code comparable problems were run on the 2D and 3D codes. Figure 12 shows the regions over which surface tractions were applied in the two codes. The 2D code was run in axisymmetric geometry and the surface traction region in the 3D code was made as nearly circular as possible.

Figure 13 compares the radial component of particle velocity between the two codes at 50 μsec while Fig. 14 compares the vertical component of particle velocity. Differences near the source are probably caused by the approximations to the circular area of loading required in the 3D simulation.

In its present form the 3D linear code is capable of determining the modification of the free field earthquake ground motion produced by a non-homogeneous geologic environment. A given equivalent source may be used to drive the 3D code in order to obtain theoretical seismograms at seismometer locations in the near field. Linking of the 3D linear code to a nonlinear code containing a stick slip rupture model is proceeding under separate funding.

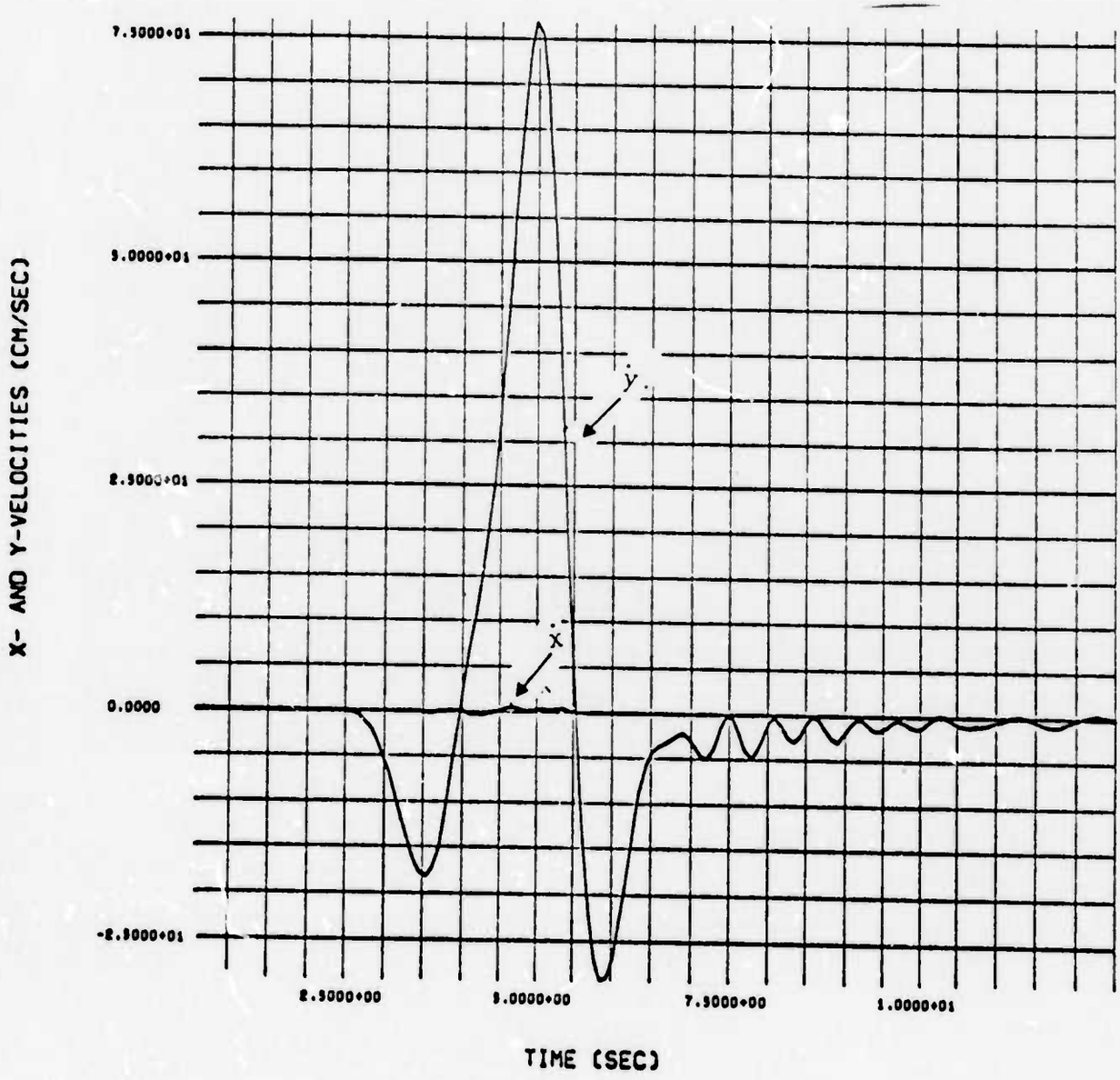

Figure 2. Particle velocity at Station 1, calculation 5A.

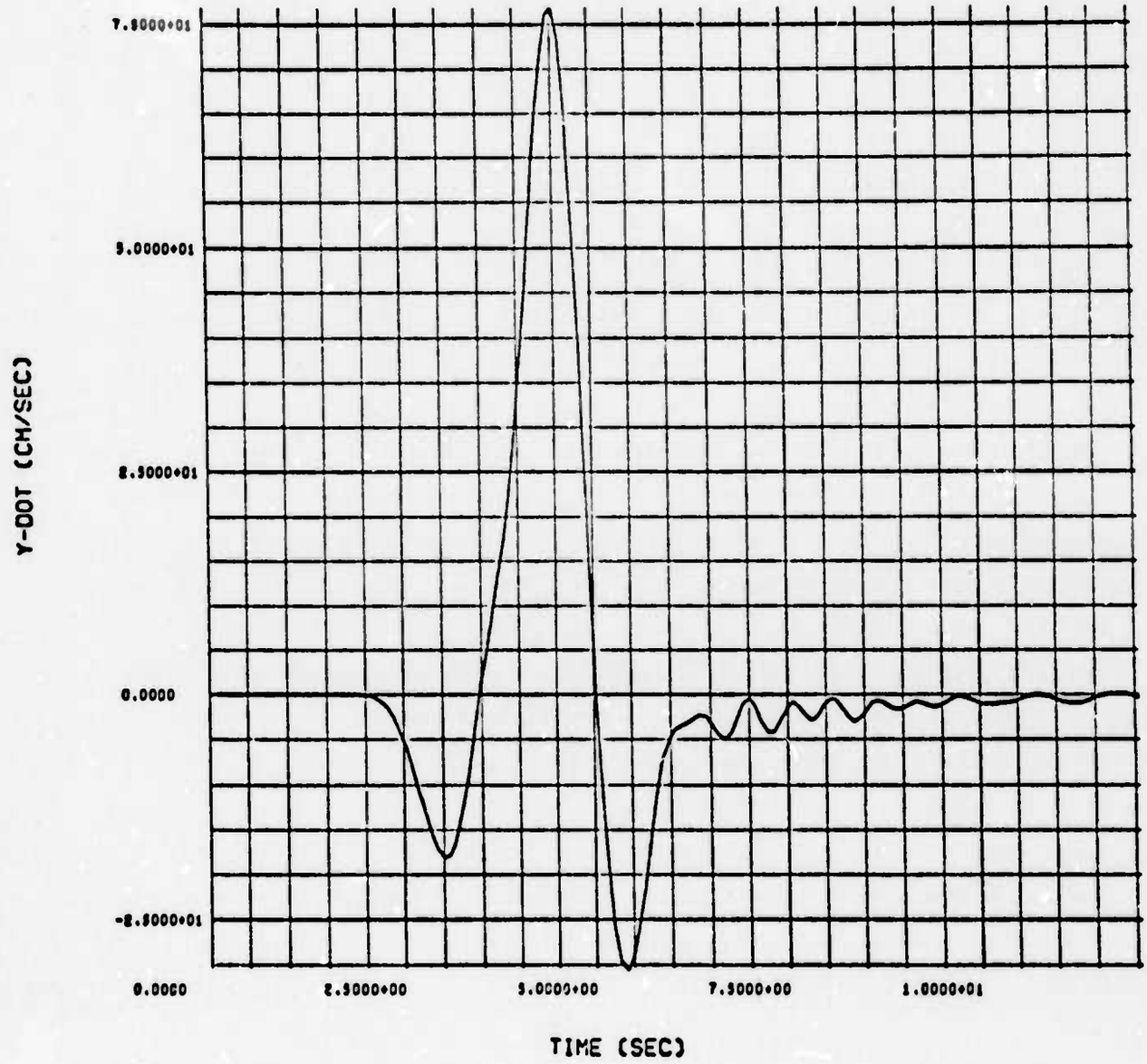

Figure 3. Particle velocity at Station 1, calculation 5A repeated with linear code linked to CRAM.

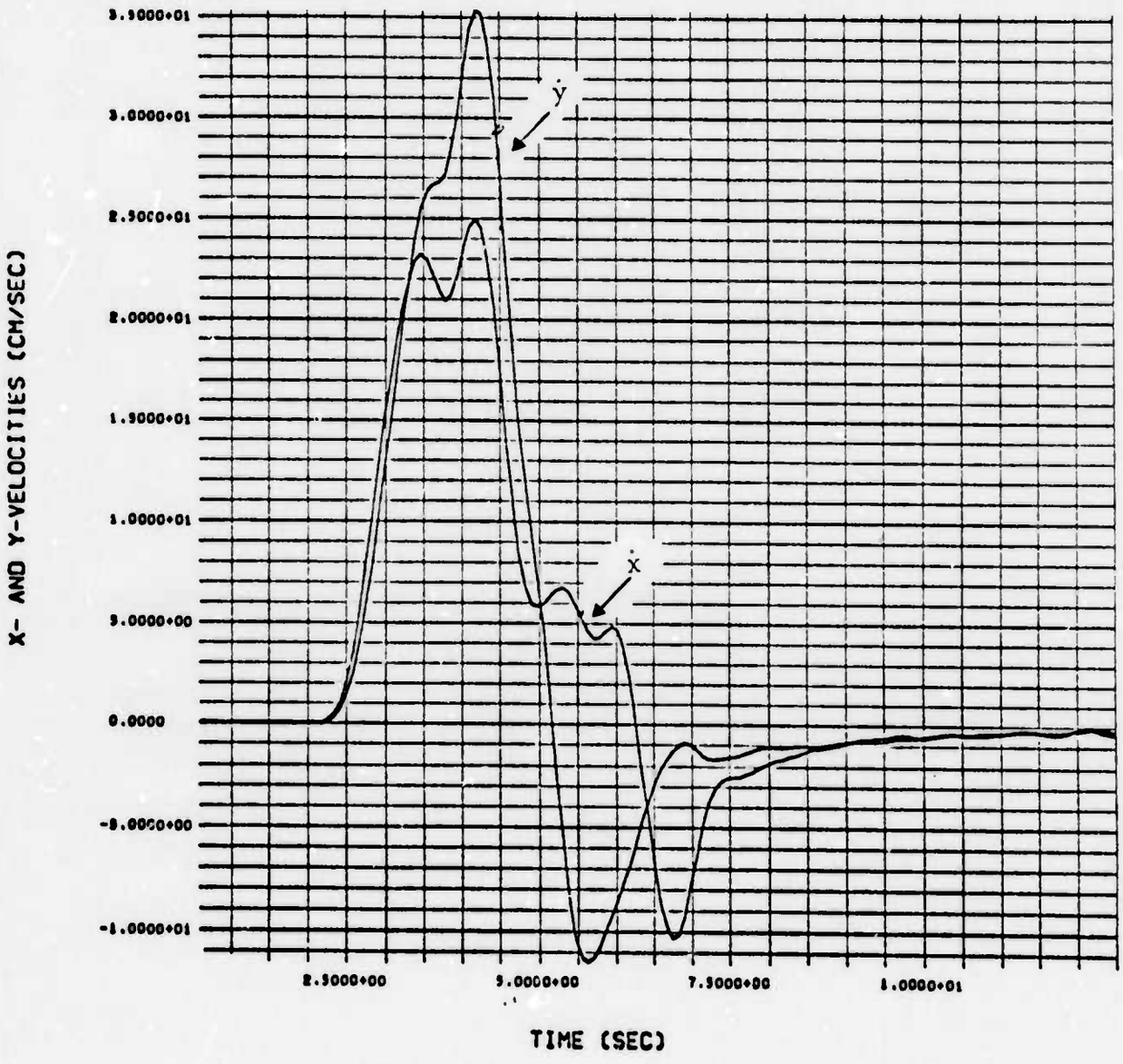

Figure 4. Particle velocity at Station 2, Calculation 5A.

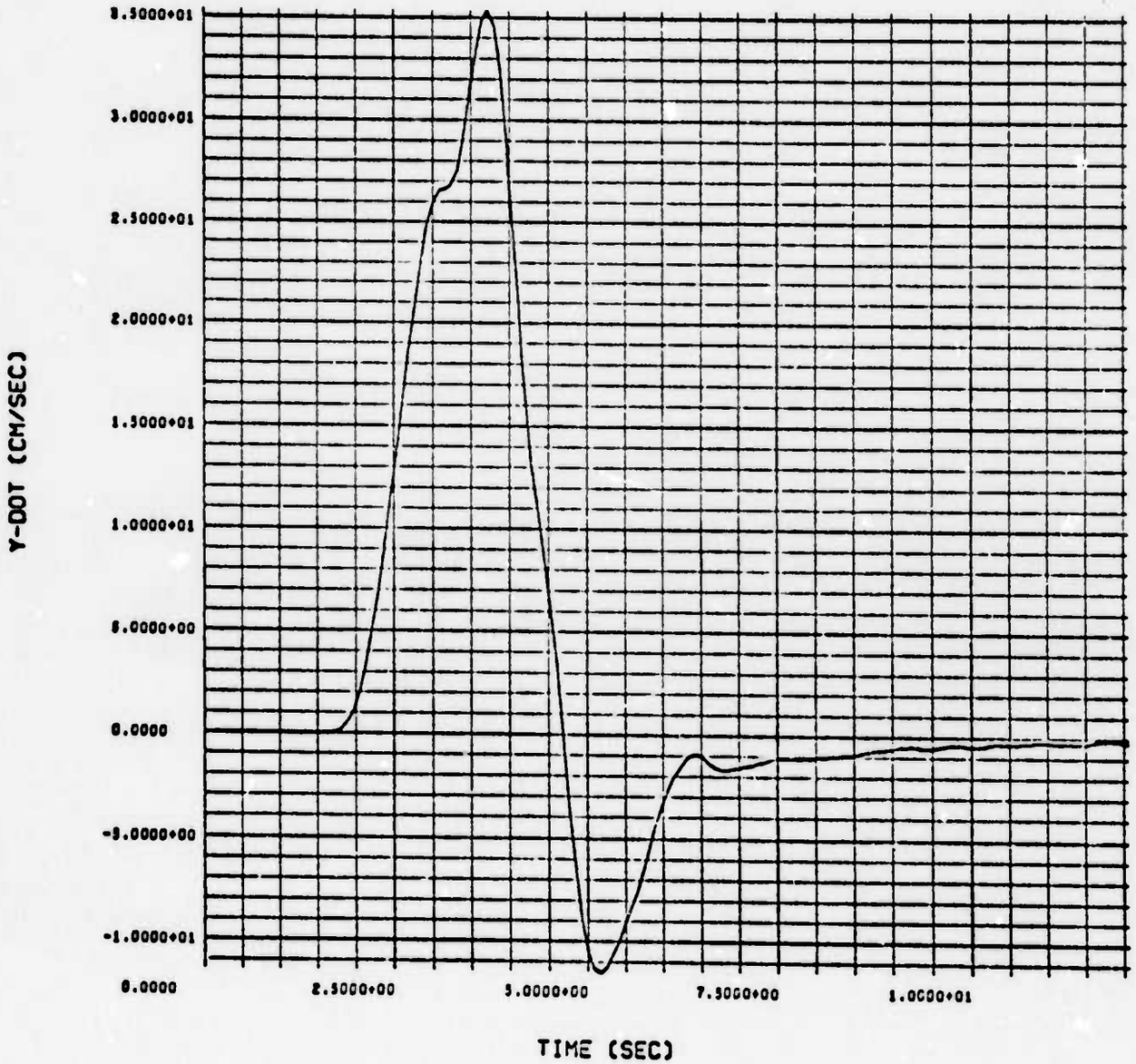

Figure 5. Particle velocity at Station 2, Calculation 5A repeated with linear code linked to CRAM.

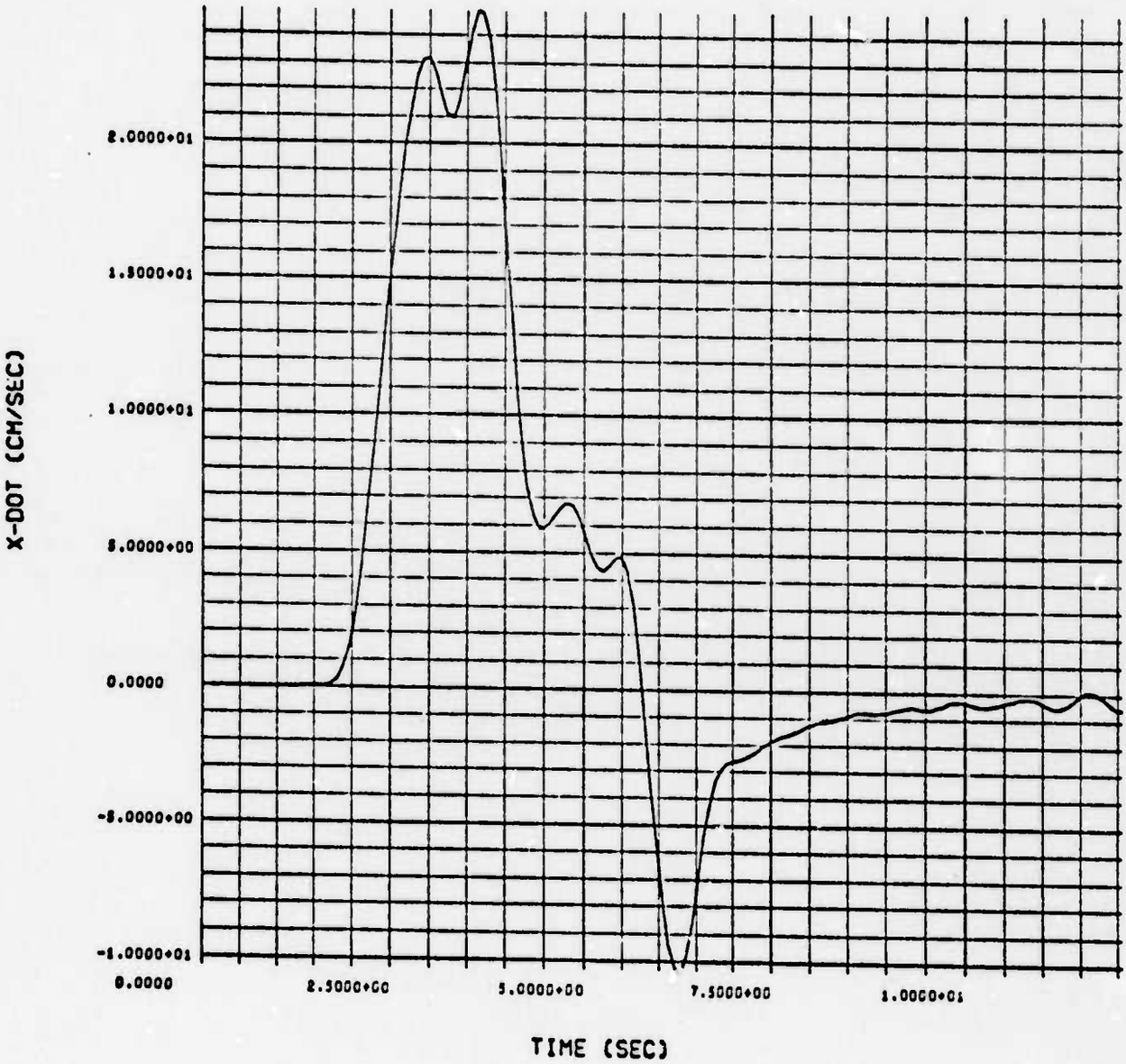

Figure 6. Particle velocity at Station 2, Calculation 5A repeated with linear code linked to CRAM.

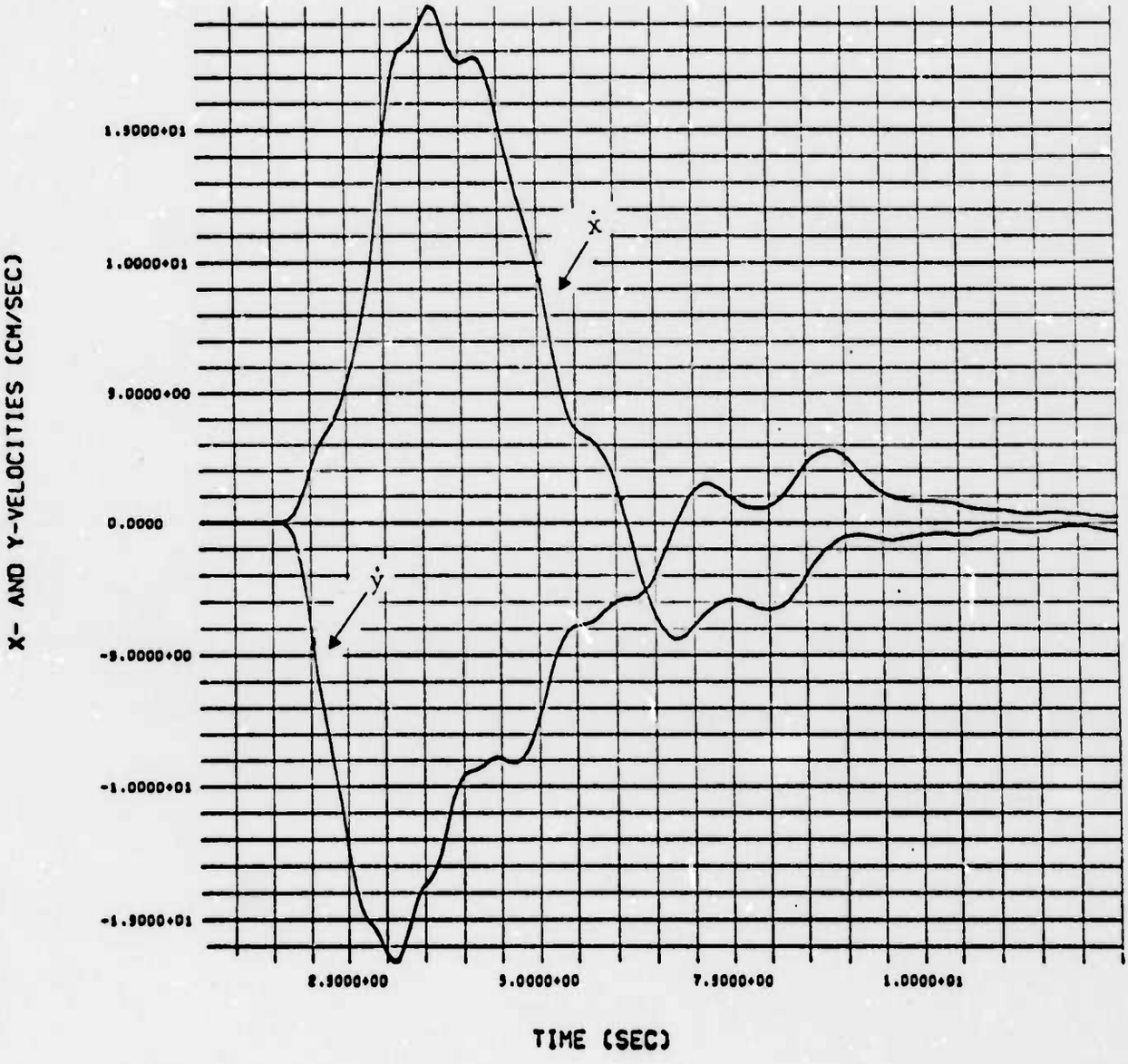

Figure 7. Particle velocity at Station 4, Calculation 5A.

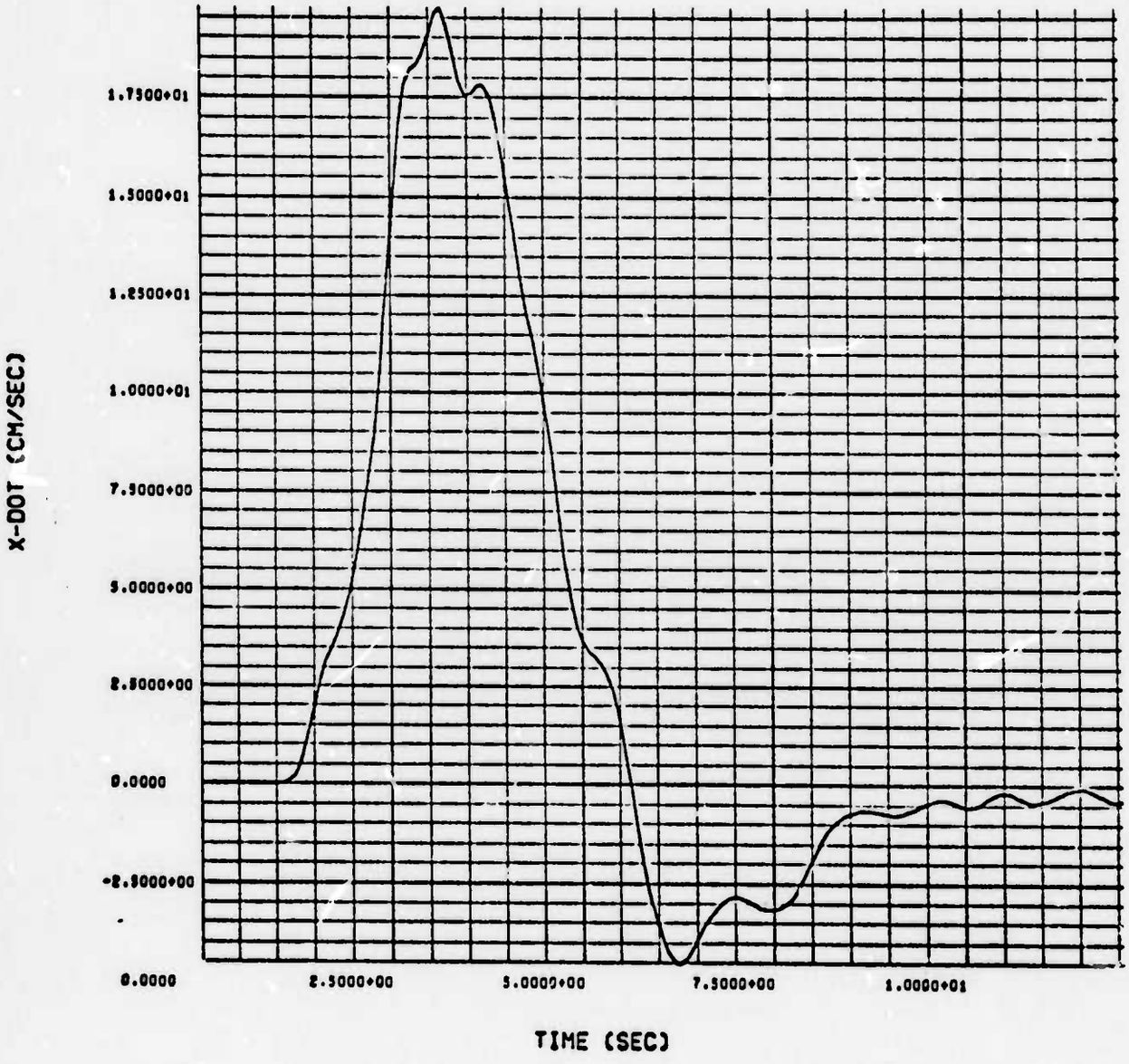

Figure 8. Particle velocity at Station 4, Calculation 5A repeated with linear code linked to CRAM.

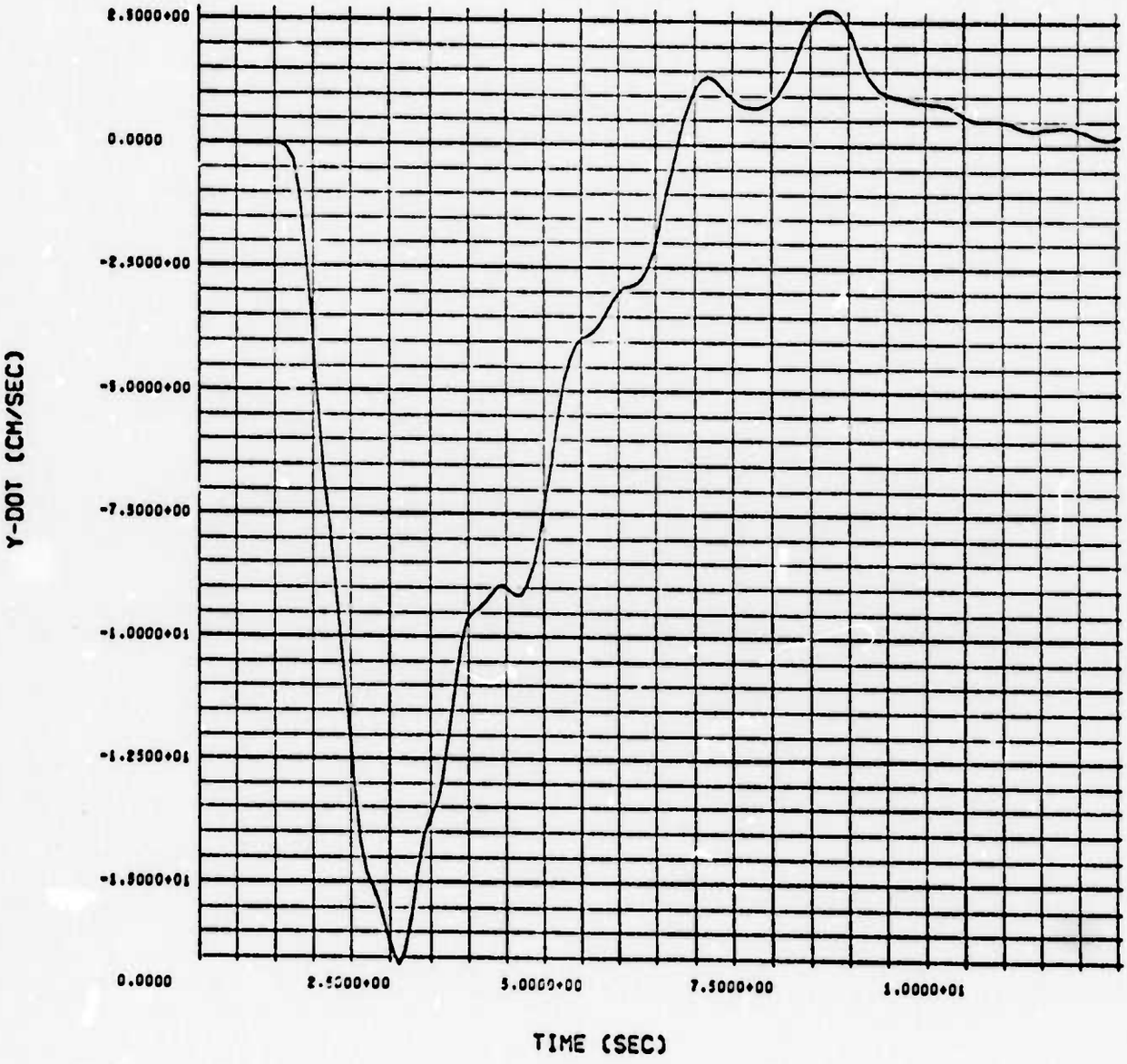

Figure 9. Particle velocity at Station 4, Calculation 5A, repeated with linear code linked to CRAM.

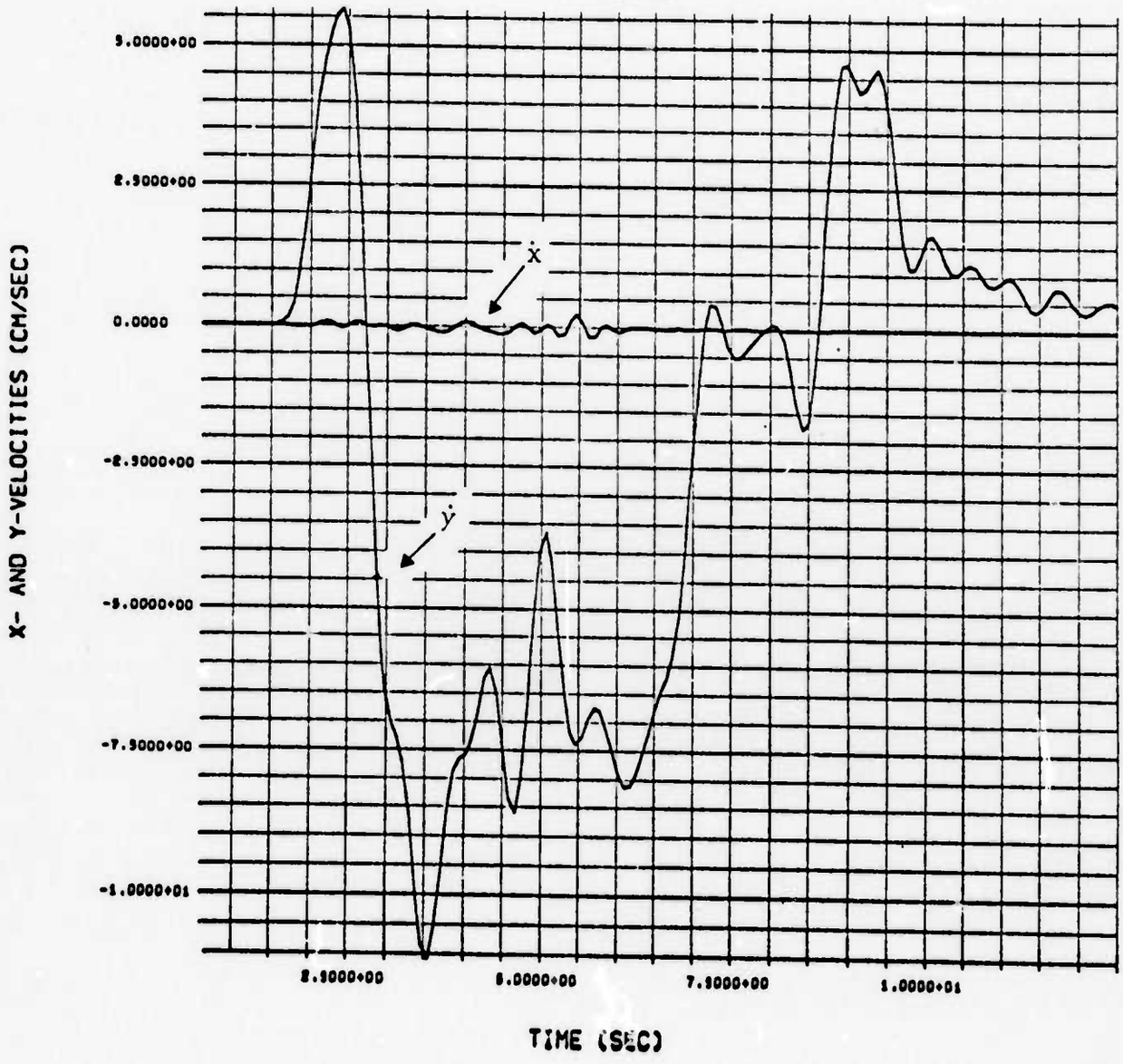

Figure 10. Particle velocity at Station 5, Calculation 5A.

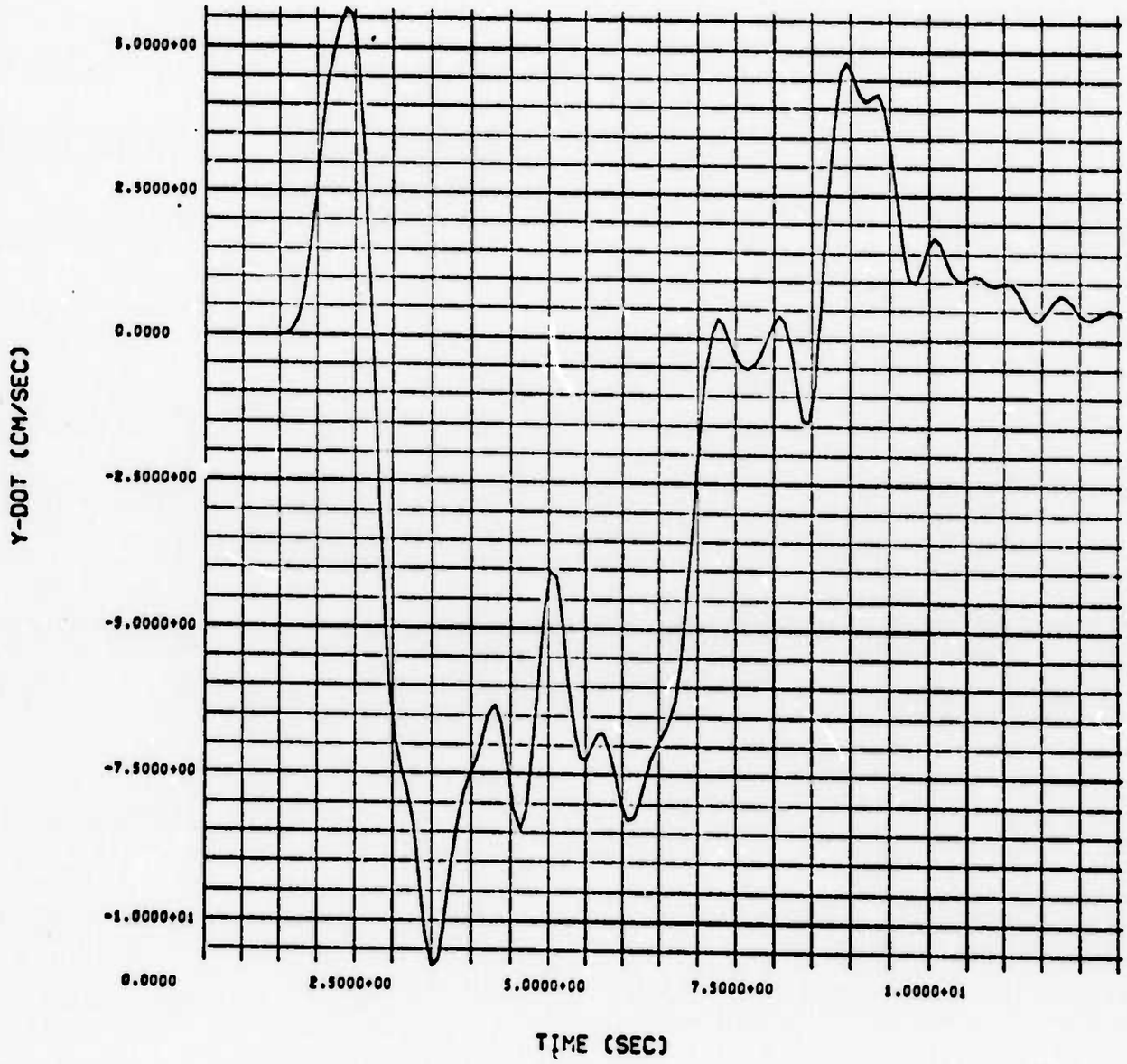

Figure 11. Particle velocity at Station 5, Calculation 5A repeated with linear code linked to CRAM.

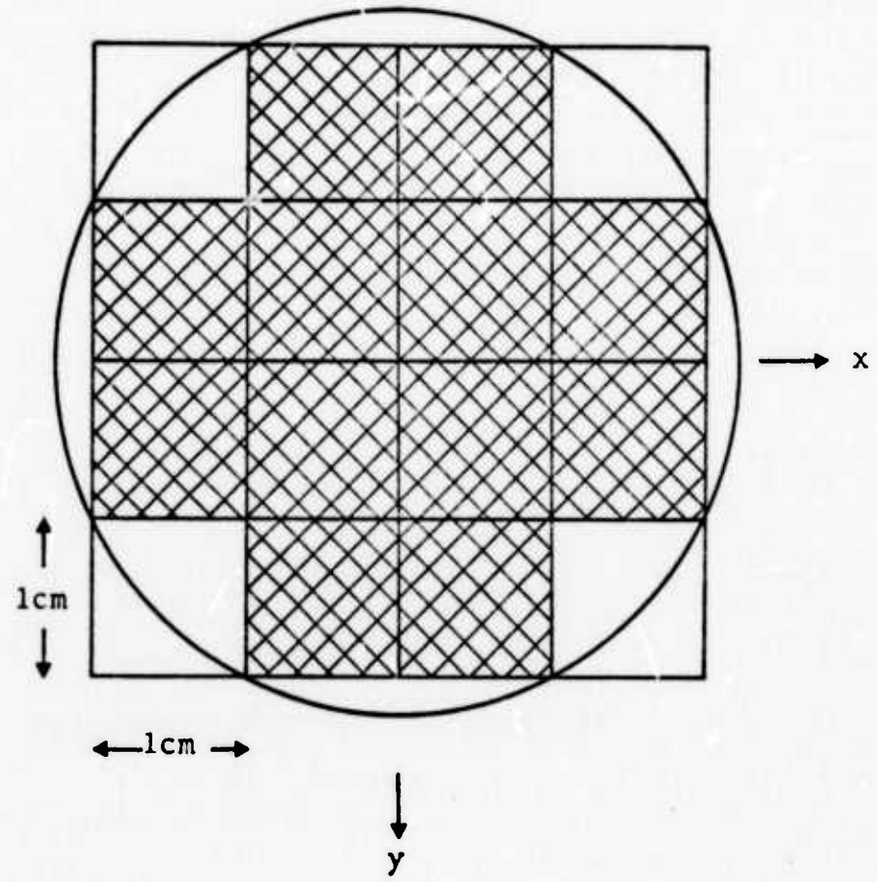

Figure 12. Surface areas over which the pressure load was applied for 2D and 3D comparison calculations. The cross hatched area corresponds to the 3D calculation.

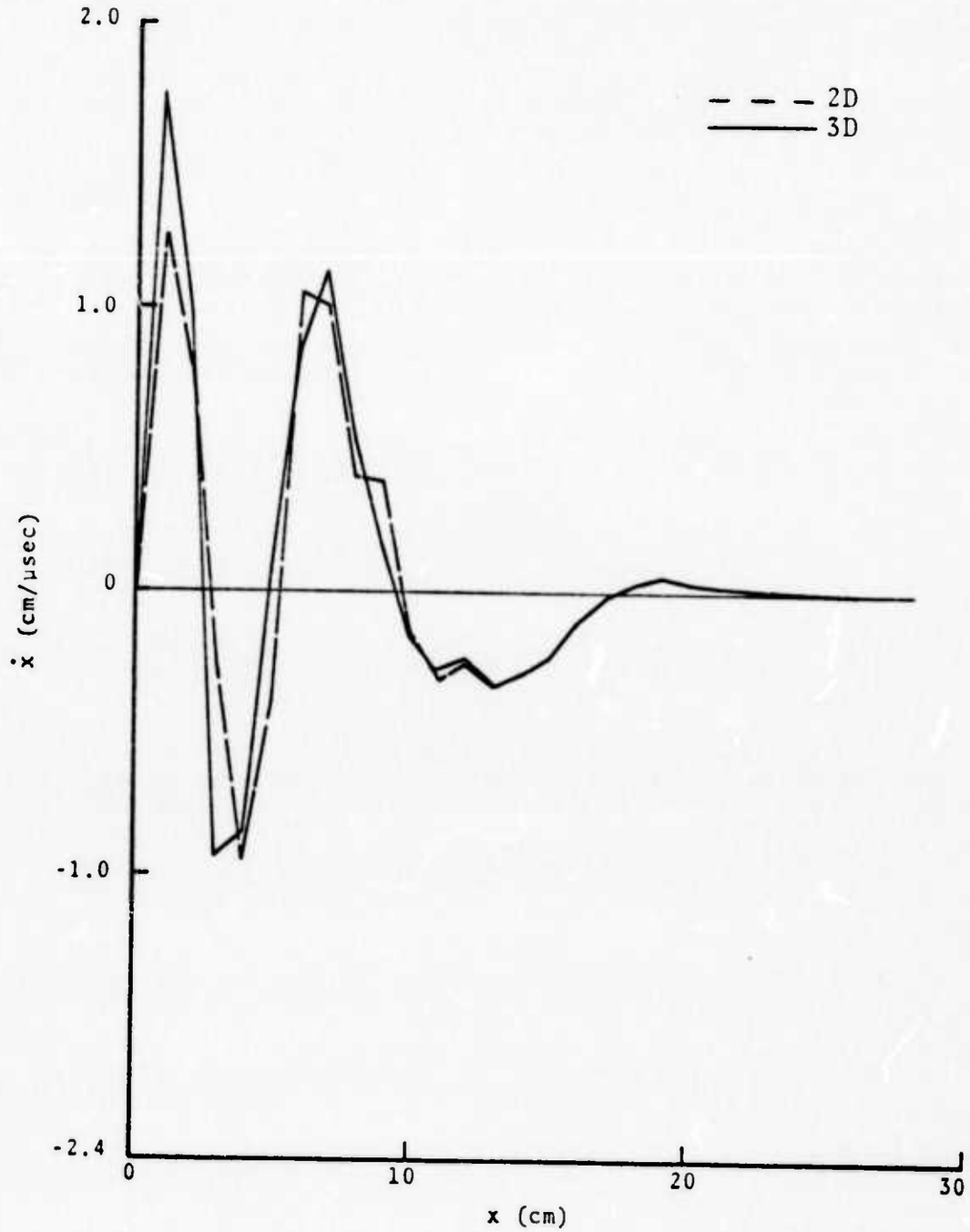

Figure 13. Comparison between 2D and 3D calculations. Radial component of particle velocity versus distance.

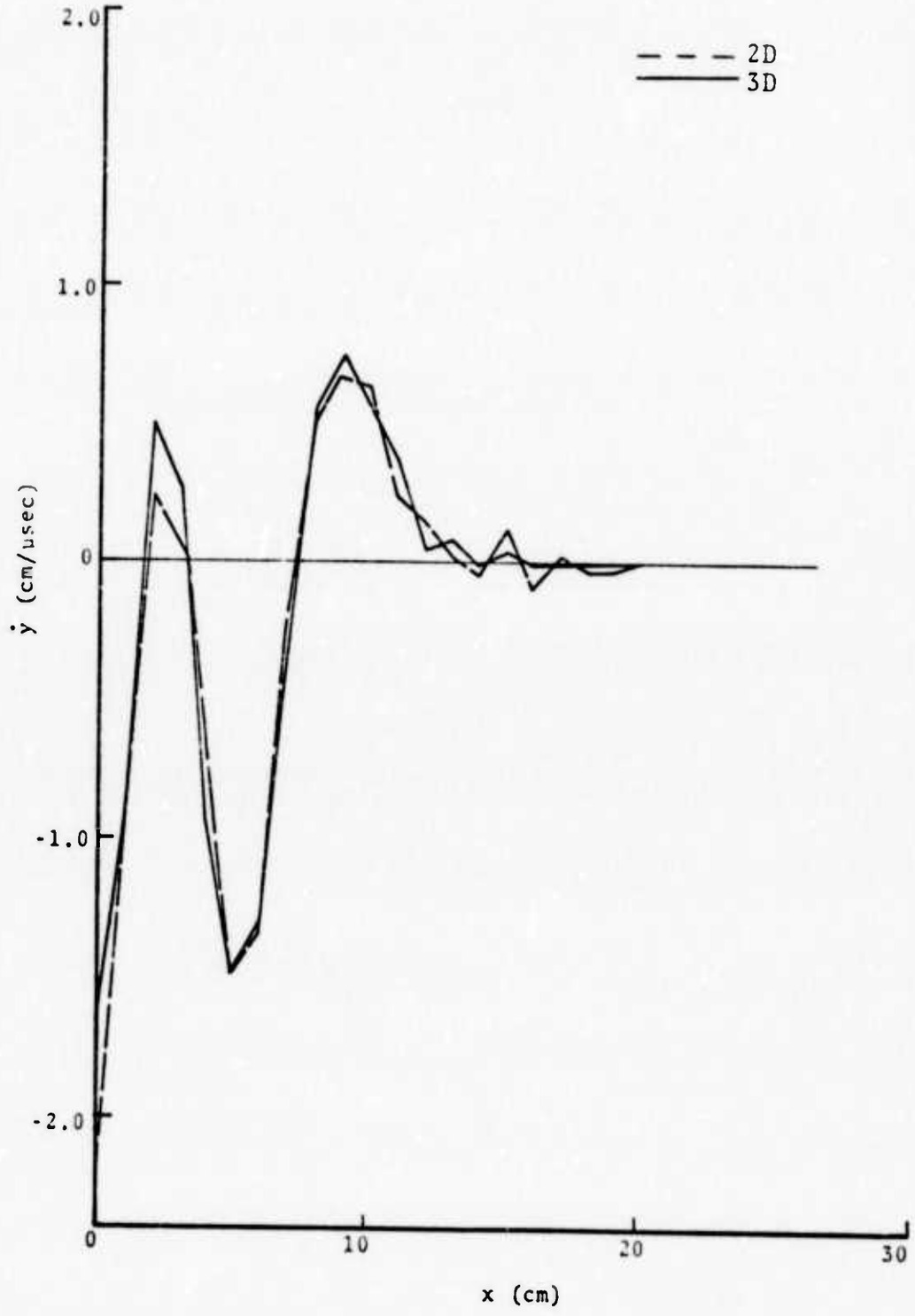

Figure 14. Comparison between 2D and 3D calculations. Vertical component of particle velocity versus distance.

REFERENCES

1. Cherry, J. T., "Calculations of Near Field, Earthquake Ground Motion," Systems, Science and Software Annual Technical Report, SSS-R-73-1759, June 29, 1973.

2. Sedgwick, R. T., and D. A. Wolfgang, "CRAM, A Two-Dimensional Lagrangian Code for Elastic-Plastic Hydrodynamic Material Behavior," General Electric Co., Report No. 695D1002, February 1969.

3. Cherry, J. T., S. Sack, G. Maenchen, and V. Kransky, "Two-Dimensional Stress Induced Adiabatic Flow," Lawrence Livermore Laboratory, UCRL-50987, 1970.

4. Wilkins, M. L., "Calculations of Elastic-Plastic Flow," in Methods in Computational Physics, Vol. 3, 1964.

APPENDIX A

The difference equations used in CRAM[2] to move an interior point are written such that the boundary conditions for an exterior point are obscured. Since we would like to isolate the normal and tangential stresses at an interior interface, this requires that the interface be treated as an exterior line over which the correct boundary stresses are applied. In this section a differencing scheme is obtained that isolates the boundary stresses and that is consistent with the CRAM interior difference equations.

The conservation of linear momentum (equation of motion) in two-dimensional Cartesian geometry is

$$\frac{d\dot{x}}{dt} = \frac{1}{\rho}\left[\frac{\partial \overline{xx}}{\partial x} + \frac{\partial \overline{xy}}{\partial y}\right] \tag{1}$$

$$\frac{d\dot{y}}{dt} = \frac{1}{\rho}\left[\frac{\partial \overline{yy}}{\partial y} + \frac{\partial \overline{xy}}{\partial x}\right] \tag{2}$$

If a Lagrangian coordinate system (k,j) is established in the material, then

$$\frac{\partial \Sigma}{\partial k} = \frac{\partial \Sigma}{\partial x}\frac{\partial x}{\partial k} + \frac{\partial \Sigma}{\partial y}\frac{\partial y}{\partial k}$$

$$\frac{\partial \Sigma}{\partial j} = \frac{\partial \Sigma}{\partial x}\frac{\partial x}{\partial j} + \frac{\partial \Sigma}{\partial y}\frac{\partial y}{\partial j}$$

where Σ is a typical stress component ($\overline{xx}$, $\overline{yy}$, $\overline{xy}$) in the equation of motion. Solving for $\partial\Sigma/\partial x$ and $\partial\Sigma/\partial y$ gives

$$\frac{\partial \Sigma}{\partial x} = \frac{1}{J}\left[\frac{\partial \Sigma}{\partial j}\frac{\partial y}{\partial k} - \frac{\partial \Sigma}{\partial k}\frac{\partial y}{\partial j}\right] \tag{3}$$

$$\frac{\partial \Sigma}{\partial y} = -\frac{1}{J}\left[\frac{\partial \Sigma}{\partial j}\frac{\partial x}{\partial k} - \frac{\partial \Sigma}{\partial k}\frac{\partial x}{\partial j}\right] \tag{4}$$

where

$$J = \frac{\partial x}{\partial j}\frac{\partial y}{\partial k} - \frac{\partial x}{\partial k}\frac{\partial y}{\partial j} \tag{5}$$

If the k,j coordinates assume discrete values

$$1, 2, \ldots k-1, k, k+1, \ldots k_{max}$$

$$1, 2, \ldots j-1, j, j+1, \ldots j_{max}$$

then

$$\vec{R}_j \times \vec{R}_k = |\vec{R}_j||R_k|\sin\alpha\ \vec{e} = 2A_a\ \vec{e} \tag{6}$$

where

$$\vec{R}_j = \frac{\partial x}{\partial j}\vec{e}_x + \frac{\partial y}{\partial j}\vec{e}_j \qquad \vec{R}_k = \frac{\partial x}{\partial k}\vec{e}_x + \frac{\partial y}{\partial k}\vec{e}_j$$

Also

$$\vec{R}_j \times \vec{R}_k = \left(\frac{\partial x}{\partial j}\frac{\partial y}{\partial k} - \frac{\partial x}{\partial k}\frac{\partial y}{\partial j}\right)\vec{e}_x \times \vec{e}_y = J\ \vec{e}_k \times \vec{e}_y \tag{7}$$

Comparing Eqs. (6) and (7) shows that a good approximation to J will be the zone area $(A_a + A_b)$ if

$$\vec{e} = \vec{e}_x \times \vec{e}_y \tag{8}$$

Equation (8) is satisfied if the x, y and k,j coordinates have the same relative orientation as that shown in Fig. 1, i.e., if the unit vector obtained from the $\vec{j} \times \vec{k}$ operation is equal to the unit vector from $\vec{e}_x \times \vec{e}_y$.

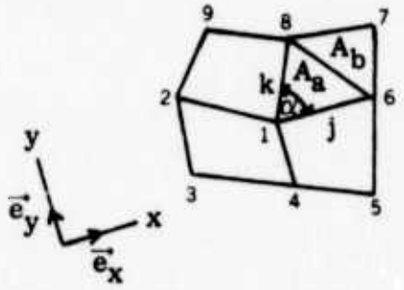

Fig. 1--The x,y and k,j coordinate system.

Figure 1 also shows the numbering system to be used for both nodal point and interior variables. Table 1 gives the equivalence between the numbering system and the k,j values.

Table 1

Number	k,j Interior	k,j Exterior
1	k-1/2, j-1/2	k,j
2		k, j-1
3		k-1, j-1
4		k-1, j
5		k-1, j+1
6	k-1/2, j+1/2	k, j+1
7	k+1/2, j+1/2	k+1, j+1
8	k+1/2, j+1/2	k+1, j
9		k+1, j-1

Typical interior variables are density, stress, strain, internal energy and area. Exterior variables are acceleration, velocity and position vector.

Equations (3) and (4) and Fig. 1 suggest a rather natural differencing scheme; i. e.,

$$\frac{1}{\rho}\frac{\partial \Sigma}{\partial x} = \frac{\Sigma_{78} y_{81}}{\frac{\rho_7 J_7 + \rho_8 J_8}{2}} w_k + \frac{\Sigma_{61} y_{14}}{\frac{\rho_6 J_6 + \rho_1 J_1}{2}} (1 - w_k) - \frac{\Sigma_{76} y_{61} w_j}{\frac{\rho_7 J_7 + \rho_6 J_6}{2}}$$

$$- \frac{\Sigma_{81} y_{12}}{\frac{\rho_8 J_8 + \rho_1 J_1}{2}} (1 - w_j) \qquad (9)$$

$$\frac{1}{\rho}\frac{\partial \Sigma}{\partial y} = -\frac{\Sigma_{78} x_{81}}{\frac{\rho_7 J_7 + \rho_8 J_8}{2}} w_k - \frac{\Sigma_{61} x_{14}}{\frac{\rho_6 J_6 + \rho_1 J_1}{2}} (1 - w_k) + \frac{\Sigma_{76} x_{61} w_j}{\frac{\rho_7 J_7 + \rho_6 J_6}{2}}$$

$$+ \frac{\Sigma_{81} x_{12}}{\frac{\rho_8 J_8 + \rho_1 J_1}{2}} (1 - w_j) \qquad (10)$$

where $\Sigma_{28} = \Sigma_7 - \Sigma_8$, $y_{81} = y_8 - y_1$, etc., and w_k and w_j weight the individual acceleration components based on their location with respect to point 1.

A fairly simple weighting scheme used in the TENSOR code[3] is

$$w_k = \frac{\vec{R}_{14} \cdot \vec{R}_{84}}{\vec{R}_{84} \cdot \vec{R}_{84}} \qquad w_j = \frac{\vec{R}_{12} \cdot \vec{R}_{62}}{\vec{R}_{62} \cdot \vec{R}_{62}}$$

In Eqs. (9) and (10), if

$$w_k = w_j = 1/2 \qquad (11)$$

$$\frac{\rho_c J_c + \rho_d J_d}{2} = \frac{\rho_1 J_1 + \rho_2 J_2 + \rho_3 J_3 + \rho_4 J_4}{4} \qquad (12)$$

then the CRAM interior differencing is obtained. Both HEMP[4] and CRAM use the same interior differencing scheme. Equations (11) and (12) reduce the TENSOR difference equations to those of CRAM and HEMP.

If a k line is to be decoupled from the grid, as in Fig. 2, then Eqs. (9) and (10) permit this if $w_k = 1$ for k^+ and $w_k = 0$ for k^-. For a point on k^+, $w_k = 1$ and $w_\ell = 1/2$. Equations (9), (10) and (12) may be used to write the spatial derivatives in Eqs. (1) and (2) giving

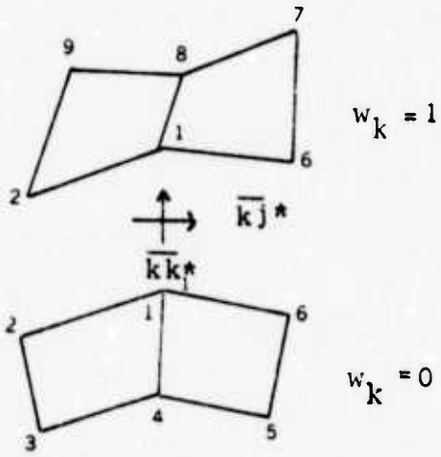

Figure 2. A decoupled interior grid line. The boundary stresses $\overline{kk}^*$ and $\overline{kj}^*$ do not change when the interface is viewed from below ($w_k = 1$) or above ($w_k = 0$).

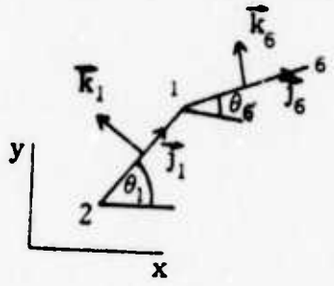

Figure 3. The orthogonal $\vec{j}$, $\vec{k}$ unit vectors.

$$\frac{1}{\rho}\frac{\partial \overline{xx}}{\partial x} = \frac{\overline{xx}_{78}\, y_{81}}{\phi^+} - \left[\frac{\left(\overline{xx}_7 - \overline{xx}^*_6\right)y_{61} + \left(\overline{xx}_8 - \overline{xx}^*_1\right)y_{12}}{\phi^+}\right] \tag{13}$$

$$\frac{1}{\rho}\frac{\partial \overline{xy}}{\partial y} = -\frac{\overline{xy}_{78}\, x_{81}}{\phi^+} + \left[\frac{\left(\overline{xy}_7 - \overline{xy}^*_6\right)x_{61} + \left(\overline{xy}_8 - \overline{xy}^*_1\right)x_{12}}{\phi^+}\right] \tag{14}$$

$$\frac{1}{\rho}\frac{\partial \overline{yy}}{\partial y} = -\frac{\overline{yy}_{78}\, x_{81}}{\phi^+} + \left[\frac{\left(\overline{yy}_7 - \overline{yy}^*_6\right)x_{61} + \left(\overline{yy}_8 - \overline{yy}^*_1\right)x_{12}}{\phi^+}\right] \tag{15}$$

$$\frac{1}{\rho}\frac{\partial \overline{xy}}{\partial x} = \frac{\overline{xy}_{78}\, y_{81}}{\phi^+} - \left[\frac{\left(\overline{xy}_7 - \overline{xy}^*_6\right)y_{61} + \left(\overline{xy}_8 - \overline{xy}^*_1\right)y_{12}}{\phi^+}\right] \tag{16}$$

where

$$\phi^+ = \frac{\rho_7 J_7 + \rho_8 J_8}{2} \tag{17}$$

Along a typical interface line joining two adjacent nodal points (Fig. 3) orthogonal unit vectors $\vec{k}$ and $\vec{j}$ are

$$\begin{aligned} \vec{k} &= -\vec{e}_x \sin\theta + \vec{e}_y \cos\theta \\ \vec{j} &= \vec{e}_x \cos\theta + \vec{e}_y \sin\theta \end{aligned} \tag{18}$$

The stress components in this coordinate system are

$$\overline{kk} = \overline{yy}\cos^2\theta + \overline{xx}\sin^2\theta - 2\overline{xy}\sin\theta\cos\theta \tag{19}$$

$$\overline{kj} = \overline{xy}(\cos^2\theta - \sin^2\theta) + (\overline{yy} - \overline{xx})\sin\theta\cos\theta \tag{20}$$

$$\overline{jj} = \overline{xx}\cos^2\theta + \overline{yy}\sin^2\theta + 2xy\sin\theta\cos\theta \tag{21}$$

The acceleration of a point on k^+ may be written as

$$\left(\frac{\dot{dx}}{dt}\right)^+ = \frac{1}{\phi^+}\left[\overline{xx}_7 y_{86} + \overline{xx}_8 y_{28} - \overline{xy}_7 x_{86} - \overline{xy}_8 x_{28} + \overline{kk}^*_6 y^+_{61} + \overline{kk}^*_1 y^+_{12} - \overline{kj}^*_6 x^+_{61} - \overline{kj}^*_1 x^+_{12}\right] \tag{22}$$

$$\left(\frac{d\dot{y}}{dt}\right)^{+} = \frac{1}{\phi^{+}}\left[-\overline{yy}_{7}x_{86} - \overline{yy}_{8}x_{28} + \overline{xy}_{7}y_{86} + \overline{xy}_{8}y_{28} - \overline{kk}^{*}_{6}x^{+}_{61} - \overline{kk}^{*}_{1}x^{+}_{12} - \overline{kj}^{*}_{6}y^{+}_{61} - \overline{kj}^{*}_{1}y^{+}_{12}\right] \quad (23)$$

Similarly, the acceleration of a point on k^{-} may be written as

$$\left(\frac{d\dot{x}}{dt}\right)^{-} = \frac{1}{\phi^{-}}\left[\overline{xx}_{6}y_{64} + \overline{xx}_{1}y_{42} - \overline{xy}_{6}x_{64} - \overline{xy}_{1}x_{42} - \overline{kk}^{*}_{6}y^{-}_{61} - \overline{kk}^{*}_{1}y^{-}_{12} + \overline{kj}^{*}_{6}x^{-}_{61} + \overline{kj}^{*}_{1}x^{-}_{12}\right] \quad (24)$$

$$\left(\frac{d\dot{y}}{dt}\right)^{-} = \frac{1}{\phi^{-}}\left[-\overline{yy}_{6}x_{64} - \overline{yy}_{1}x_{42} + \overline{xy}_{6}y_{64} + \overline{xy}_{1}y_{42} + \overline{kk}^{*}_{6}x^{-}_{61} + \overline{kk}^{*}_{1}x^{-}_{12} + \overline{kj}^{*}_{6}y^{-}_{61} + \overline{kj}^{*}_{1}y^{-}_{12}\right] \quad (25)$$

These equations have been derived assuming that $\overline{kk}^{*}_{6}$, $\overline{kj}^{*}_{6}$, $\overline{kk}^{*}_{1}$ and $\overline{kj}^{*}_{1}$ are specified along the 6-2 interface, finding the corresponding stresses in the x,y coordinate system, i.e.,

$$\overline{xx}^{*} = \overline{jj}^{*}\cos^{2}\theta + \overline{kk}^{*}\sin^{2}\theta - 2\overline{kj}^{*}\sin\theta\cos\theta \quad (26)$$

$$\overline{yy}^{*} = \overline{jj}^{*}\sin^{2}\theta + \overline{kk}^{*}\cos^{2}\theta + 2\overline{kj}^{*}\sin\theta\cos\theta \quad (27)$$

$$\overline{xy}^{*} = (\overline{jj}^{*} - \overline{kk}^{*})\sin\theta\cos\theta + \overline{jk}^{*}(\cos^{2}\theta - \sin^{2}\theta) \quad (28)$$

and then substituting these expressions for $\overline{xx}^{*}_{6}$, $\overline{yy}^{*}_{6}$, $\overline{xy}^{*}_{6}$, $\overline{xx}^{*}_{1}$, $\overline{yy}^{*}_{1}$, $\overline{xy}^{*}_{1}$ into Eqs. (13) through (16)

Equations (22) through (25) will be used to move the points on the decoupled grid line. They are consistent with the interior difference equations.

APPENDIX B

In order to use Equations 22 through 25 in Appendix A the boundary stresses must be specified. In order to solve for these stresses we apply contact discontinuity boundary conditions, which require that the normal component of stress and normal component of velocity be continuous at the boundary.

The unit vectors normal and tangent to the 6-2 interface may be written

$$\begin{aligned} \vec{k} &= -\sin\theta\ \vec{e}_x + \cos\theta\ \vec{e}_y \qquad & \vec{e}_x &= -\sin\theta\ \vec{k} + \cos\theta\ \vec{j} \\ \vec{j} &= \cos\theta\ \vec{e}_x + \sin\theta\ \vec{e}_y \qquad & \vec{e}_y &= \cos\theta\ \vec{k} + \sin\theta\ \vec{j} \end{aligned} \tag{1}$$

The acceleration components on the plus side of the line may be written

$$a_k^+ = \frac{1}{\phi^+}\left[g_k^+ + R_{61}\,\overline{kk}_7 + R_{12}\,\overline{kk}_\theta - (R_{61}+R_{12})\,\overline{kk}^*\right] \tag{2}$$

$$a_j^+ = \frac{1}{\phi^+}\left[g_j^+ + R_{61}\,\overline{kj}_7 + R_{12}\,\overline{kj}_\theta - (R_{61}+R_{12})\,\overline{kj}^*\right] \tag{3}$$

The corresponding acceleration components on the minus side are

$$a_k^- = \frac{1}{\phi^-}\left[g_k^- + (R_{61}+R_{12})\,\overline{kk}^* - R_{61}\,\overline{kk}_6 - R_{12}\,\overline{kk}_1\right] \tag{4}$$

$$a_j^- = \frac{1}{\phi^-}\left[g_j^- + (R_{61}+R_{12})\,\overline{kj}^* - R_{61}\,\overline{kj}_6 - R_{12}\,\overline{kj}_1\right] \tag{5}$$

where

$$g_k^+ = -(\overline{xx}_{78}y_{81} - \overline{xy}_{78}x_{81})\sin\theta - (\overline{yy}_{78}x_{81} - \overline{xy}_{78}y_{81})\cos\theta \quad (6)$$

$$g_k^- = -(\overline{xx}_{61}y_{14} - \overline{xy}_{61}x_{14})\sin\theta - (\overline{yy}_{61}x_{14} - \overline{xy}_{61}y_{14})\cos\theta$$

$$g_j^+ = (\overline{xx}_{78}y_{81} - \overline{xy}_{78}x_{81})\cos\theta - (\overline{yy}_{78}x_{81} - \overline{xy}_{78}y_{81})\sin\theta \quad (7)$$

$$g_j^- = (\overline{xx}_{61}y_{14} - \overline{xy}_{61}x_{14})\cos\theta - (yy_{61}x_{14} - \overline{xy}_{61}y_{14})\sin\theta$$

$$\phi^+ = \frac{1}{2}\left[\rho_7 J_7 + \rho_8 J_8\right] \qquad \phi^- = \frac{1}{2}\left[\rho_6 J_6 + \rho_1 J_1\right] \quad (8)$$

Equations 2 through 5 have been derived from Equations 13 through 16 in Appendix A by assuming that the boundary stress is uniform over the entire 6-2 portion of the grid line. These equations, therefore, are not completely consistent with the interior difference equations. The assumption concerning uniform boundary stress is necessary since the contact discontinuity boundary conditions will result in an equation that relates the normal components of acceleration on the plus and minus side of the boundary. This equation should contain only one unknown, i.e., the normal component of the boundary stress.

In order to find the relation between the above acceleration components at a slipping interface, we follow the technique used by Cherry, et al.[3] and attach a coordinate system to the point on the minus side, with $\vec{k}$ and $\vec{j}$ being the unit vectors normal and tangent to the slip line at the point to be moved.

If $\vec{v}^{+}$ and $\vec{v}^{-}$ are the velocities on the plus and minus side of the slip line then, from Equation 1, the normal components of velocity are given by

$$\begin{aligned} \vec{v}^{+} \cdot \vec{k} &= -\dot{x}^{+} \sin\theta + \dot{y}^{+} \cos\theta \\ v^{-} \cdot \vec{k} &= -\dot{x}^{-} \sin\theta + \dot{y}^{-} \cos\theta \end{aligned} \tag{9}$$

If

$$x_{\ell}^{-} = \frac{\partial x^{-}}{\partial \ell} \qquad y_{\ell}^{-} = \frac{\partial y^{-}}{\partial \ell} \qquad R_{\ell} = \left[\left(x_{\ell}^{-} \right)^2 + \left(y_{\ell}^{-} \right)^2 \right]^{1/2}$$

then

$$\sin\theta = \frac{y_{\ell}^{-}}{R_{\ell}} \qquad \cos\theta = \frac{x_{\ell}^{-}}{R_{\ell}} \tag{10}$$

Substituting Equation 10 into 9, and equating normal velocity components gives

$$R_{\ell} \vec{v}^{-} \cdot \vec{k} = R_{\ell} \vec{v}^{+} \cdot k \tag{11}$$

or

$$-\dot{x}^{-} y_{\ell}^{-} + \dot{y}^{-} x_{\ell}^{-} = -\dot{x}^{+} y_{\ell}^{-} + \dot{y}^{+} x_{\ell}^{-} \tag{12}$$

Since the $\vec{k},\vec{\ell}$ coordinate system is attached to the minus side of the slip line then

$$\frac{d}{dt} \left(-\dot{x}^{-} y_{\ell}^{-} + \dot{y}^{-} x_{\ell}^{-} \right) = \frac{\partial}{\partial t} \left(-\dot{x}^{+} y_{\ell}^{-} + \dot{y}^{+} x_{\ell}^{-} \right) \Big|_{k,\ell \text{ constant}} \tag{13}$$

The left side of Equation 13 may be written

$$-y_\ell^- \frac{d}{dt}(\dot{x}^-) + x_\ell^- \frac{d}{dt}\dot{y}^- - \dot{x}^-\dot{y}_\ell^- + \dot{y}^-\dot{x}_\ell^-$$

$$= R_\ell a_k^- + (\vec{v}^- \cdot \vec{k})(\vec{v}_\ell^- \cdot \vec{j}) - (\vec{v}^- \cdot \vec{\ell})(\vec{v}_\ell^- \cdot \vec{k}) \tag{14}$$

Since

$$\frac{d}{dt}(R_\ell v^+ \cdot \vec{k}) = \frac{\partial}{\partial t}(R_\ell v^+ \cdot \vec{k}) + \frac{(v^+ - v^-)}{R_\ell} \cdot \vec{\ell}\, \frac{\partial}{\partial \ell}(R_\ell \vec{v}^+ \cdot \vec{k})$$

$$+ \frac{(v^+ - v^-)\cdot \vec{k}}{R_k} \frac{\partial}{\partial k}(\vec{R}_\ell \vec{v}^+ \cdot \vec{k})$$

and

$$(v^+ - \vec{v}) \cdot \vec{k} = 0$$

Then the right side of Equation 13 may be written

$$\frac{\partial}{\partial t}(-\dot{x}^+ y_\ell^- + \dot{y}^+ x_\ell^-)$$

$$= R_\ell a_k^+ + (\vec{v}^+ \cdot \vec{k})(\vec{v}_\ell^- \cdot \vec{j}) - (\vec{v}^- \cdot \vec{\ell})(\vec{v}_\ell^- \cdot \vec{k}) - (v^+ - v^-)\cdot \vec{\ell}\, \vec{v}_\ell^+ \cdot \vec{k} \tag{15}$$

In Equations 14 and 15 a_k^+ and a_k^- are given by

$$a_k^+ = -\frac{d(\dot{x}^+)}{dt}\frac{y_\ell^-}{R_\ell} + \frac{d(\dot{y}^+)}{dt}\frac{y_\ell^-}{R_\ell}$$

$$a_k^- = -\frac{d(\dot{x}^-)}{dt}\frac{y_\ell^-}{R_\ell} + \frac{d(\dot{y}^-)}{dt}\frac{y_\ell^-}{R_\ell}$$

and are the same acceleration components given by Equations 2 and 4. We have also used the relation

$$-\dot{x}^{\pm}\dot{y}_{\ell}^{-}+\dot{y}^{\pm}\dot{x}_{\ell}^{-} = (\vec{v}^{\pm}\cdot\vec{k})(\vec{v}_{\ell}^{-}\cdot\vec{j}) - (\vec{v}^{\pm}\cdot\vec{\ell})(v_{\ell}^{-}\cdot\vec{k}) \qquad (16)$$

in order to derive Equations 14 and 15.

Substituting Equations 14 and 15 into Equation 13 gives

$$a_k^{+}-a_k^{-} = A_c \qquad (16)$$

where

$$A_c = \frac{(\vec{v}^{+}-\vec{v}^{-})\cdot\vec{\ell}\,(\vec{v}_{\ell}^{+}+\vec{v}_{\ell}^{-})\cdot\vec{k}}{R_{\ell}} \qquad (17)$$

Solving Equation 16 for $\overline{kk}^*$ gives

$$\overline{kk}^* = \frac{\phi^{-}g_k^{+}-\phi^{+}g_k^{-} + \phi^{-}(R_{61}\overline{kk}_7+R_{12}\overline{kk}_8) + \phi^{+}(R_{61}\overline{kk}_6+R_{12}\overline{kk}_1) - \phi^{+}\phi^{-}A_c}{(R_{61}+R_{12})(\phi^{+}+\phi^{-})} \qquad (18)$$

Equation 18 relates the normal component of stress ($\overline{kk}^*$) at the slipping interface to interior zone variables. In order to move the boundary points then $\overline{kj}^*$ in Equations 22 through 24 in Appendix A must also be specified.

For a tied point A_c in Equation 18 is set equal to zero, since

$$(\vec{v}^{+}-\vec{v}^{-})\cdot\vec{\ell} = 0 \quad .$$

Also the tangential stress component, for a tied point, is obtained from Equations 3 and 5. Since

$$a_j^+ = a_j^-$$

then for a tied point

$$\overline{kj}^* = \frac{\phi^- g_j^+ - \phi^+ g_j^- + \phi^- (R_{61}\,\overline{kj}_7 + R_{12}\,\overline{kj}_8) + \phi^+ (R_{61}\,\overline{kj}_6 + R_{12}\,\overline{kj}_1)}{(R_{61}+R_{12})(\phi^+ + \phi^-)} \quad (19)$$

APPENDIX C

Plastic flow is due to the inability of real materials to support unlimited values of shear stress. In the code the deviatoric stress components are modified such that the resulting stress state is consistent with a Mises yield criterion.

If the second deviatoric invariant (J) is greater than a specified value ($1/3\ Y^2$), then

$$S_{ij} = \hat{S}_{ij} \frac{Y}{\sqrt{3J}} \left(J > \frac{Y^2}{3} \right) \tag{1}$$

where S_{ij} is the adjusted stress deviator

$\hat{S}_{ij}$ is the stress deviator calculated by assuming that the total strain rate is elastic, and

$$J = \frac{1}{2} (\hat{S}_{ij} \hat{S}_{ji}) \tag{2}$$

For a triaxial test, Y corresponds to the maximum allowable stress difference at failure.

Rupture initiation is being modeled by accumulating the difference between $\sqrt{3J}$ and Y during yielding. When this accumulation reaches a specified value then the point at the fault surface enters the slip routine. Between two consecutive cycles, n and n+1, the accumulation takes the form

$$\begin{aligned} e^{n+1} &= e^n + \frac{\sqrt{3J} - Y}{Y}, \quad \left(J > \frac{Y^2}{3} \right) \\ e^{n+1} &= e^n \qquad\qquad \left(J \leq \frac{Y^2}{3} \right) \end{aligned} \tag{3}$$

Rupture occurs if

$$e^{n+1} \geq W \tag{4}$$

where W is a specified function of distance from the initial point of rupture (the focus).

Equation (3) is similar to a plastic work criterion, where the plastic work (E^{n+1}) is given by

$$E^{n+1} = E^n + \frac{Y^2}{3\mu} \frac{\sqrt{3J} - Y}{Y} \tag{5}$$

Equations (3) and (5) differ only by the factor $Y^2/3\mu$.

We have been successful in both controlling rupture velocity and reducing the stress concentrations at the end of the fault by allowing W, in Eq. (4), to be a specified function of distance from the point of rupture initiation. The functional form that has been used is

$$W = 6c\left(\frac{x + L/2}{d}\right)^2\left[\frac{1}{2} - \frac{1}{3}\frac{x + L/2}{d}\right] \qquad 0 \leq x + \frac{L}{2} \leq \frac{1}{2} \tag{6a}$$

$$= \frac{c}{2}\left[-\frac{1}{2} + 3\frac{x + L/2}{d}\right] \qquad x + \frac{L}{2} \geq \frac{d}{2} \tag{6b}$$

where L, c and d are input parameters. The rupture is constrained to lie between $-L/2 \leq x \leq L/2$, where L is the fault length.

APPENDIX D

LINEAR DIFFERENCING SCHEME USED IN LAGS

The following discussion concerns the differencing scheme used in the finite difference stress wave code LAGS. This code performs the Linear Analysis of Geologic Structures. The differencing is similar to that originally presented by Wilkins[4] and also used in CRAM.[2] In this scheme the equilibrium equations containing the stresses and their spatial partial derivatives are differenced. The stress-displacement relationships are differenced separately to complete the finite-difference formulation. This procedure is superior to differencing the equilibrium equations written in terms of displacements for two important reasons. First, this procedure allows the treatment of almost any non-uniform material description. Second, boundary condition incorporation is facilitated using this technique. Both axisymmetric and plane strain configurations can be considered.

The dynamic equilibrium equations in the (x,y) Cartesian coordinate system are given by

$$\rho\ddot{u} = \frac{\partial\sigma_x}{\partial x} + \frac{\partial\sigma_{xy}}{\partial y} + \frac{\sigma_x - \sigma_\theta}{x}\Bigg|^* \qquad (1)$$

$$\rho\ddot{v} = \frac{\partial\sigma_{xy}}{\partial x} + \frac{\partial\sigma_y}{\partial y} + \frac{\sigma_{xy}}{x}\Bigg|^* .$$

where (u,v) are the displacements in the (x,y) directions, dots denote time derivatives, ρ is the density, θ is the circumferential direction, and σ_{mn} is the stress tensor. The * quantities are non-zero for axisymmetric configurations only. The first step in the determination of an approximate solution of Eq. (1) is to

divide the continuum into a discrete number of nodes. As depicted in Fig. 1, these points are identified in the two-dimensional space by their i and j values. The program LAGS assumes a rectilinear mesh geometry. The Dx_i and Dy_j increments describing this geometry (see Fig. 1) may be non-uniform and are supplied by the user. In addition, each cell in the mesh must be supplied a material identifier. This flexibility allows the treatment of almost any general geologic structure.

If Dt is the time increment and t^n a discrete value of time (equal to nDt), the time differenced representation of Eq. (1) is based on the following analog:

$$\begin{aligned} \dot{a}^{n+\frac{1}{2}} &= \dot{a}^{n-\frac{1}{2}} + Dt\ddot{a}^n \\ a^{n+1} &= a^n + Dt\dot{a}^{n+\frac{1}{2}} , \end{aligned} \tag{2}$$

where a is u or v. The spatial difference analogs at a particular (i,j) node which are required to simulate Eq. (1) are of the following form:[2,4]

$$\begin{aligned} \left(\frac{1}{\rho}\frac{\partial A}{\partial x}\right)_{i,j} &= \frac{2}{\phi_{i,j}}\left(A_1\Delta y_1 - A_2\Delta y_2 - A_3\Delta y_3 + A_4\Delta y_4\right)_{i,j} \\ \left(\frac{1}{\rho}\frac{\partial A}{\partial y}\right)_{i,j} &= \frac{2}{\phi_{i,j}}\left(A_1\Delta x_1 + A_2\Delta x_2 - A_3\Delta x_3 - A_4\Delta x_4\right)_{i,j} \end{aligned} \tag{3}$$

where the subscript n refers to the n^{th} cell of Fig. 1 and A is some component of stress. The terms $\phi_{i,j}$, Δx_n, and Δy_n are defined by:

$$\begin{aligned} \phi_{i,j} &= \sum_{k=1}^{4} \rho_k \Delta x_k \Delta y_k \\ \Delta x_1 &= \Delta x_4 = Dx_{i+1} \\ \Delta x_2 &= \Delta x_3 = Dx_i \end{aligned} \tag{4}$$

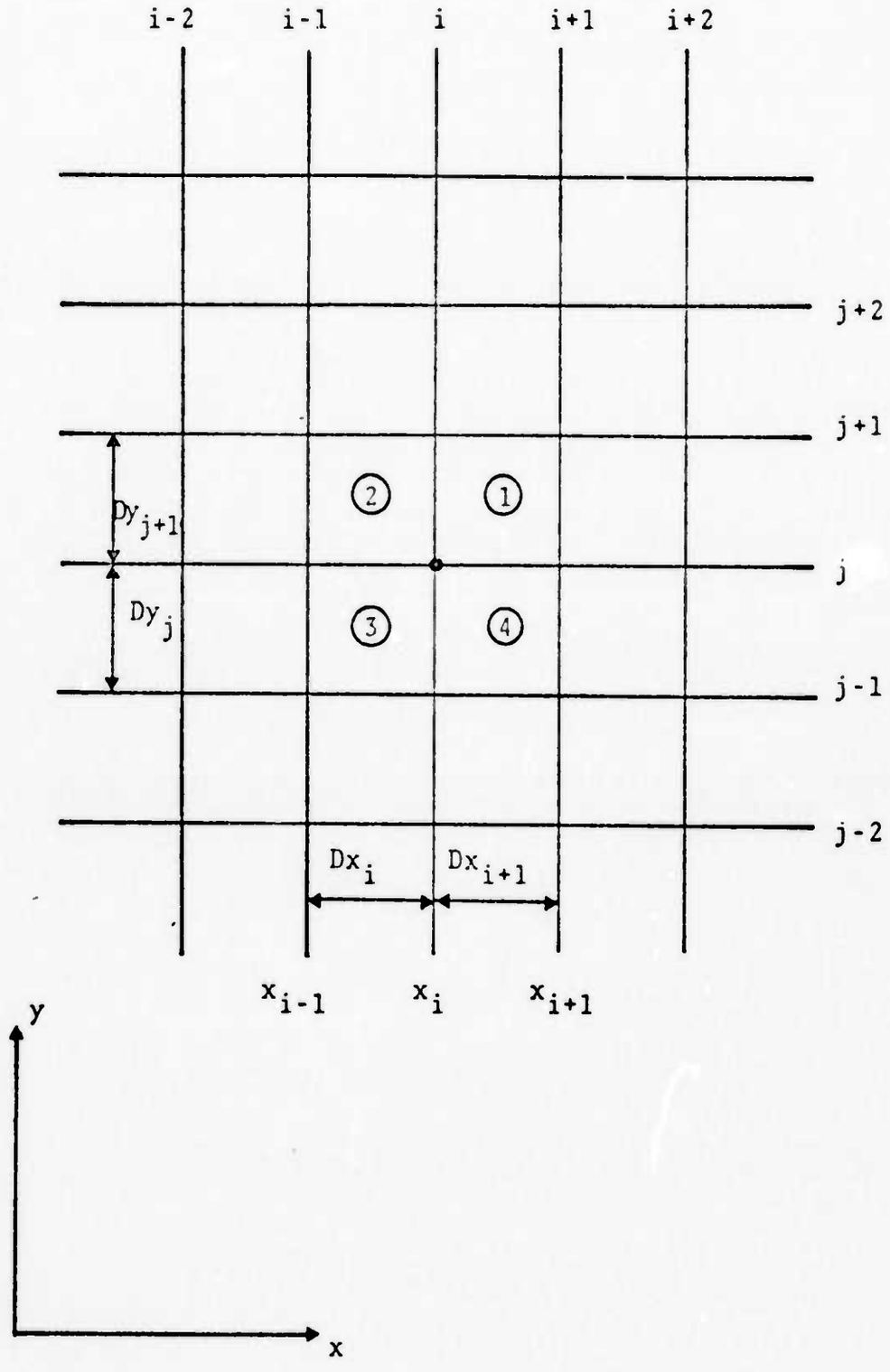

Figure 1. Geometry of (i,j) grid configuration.

in a linear isotropic media are related by

$$\sigma_{mn} = \lambda \varepsilon_{kk} \delta_{mn} + 2\mu \varepsilon_{mn}, \tag{6}$$

where λ and μ are the Lame´ constans, δ_{mn} is the Krönecker delta function, ε_{mn} is the strain tensor, and double subscripts denote summation. In this case

$$\varepsilon_{kk} = \varepsilon_x + \varepsilon_y + \varepsilon_\theta.$$

The linear strain-displacement relationships are given by

$$\begin{aligned}
\varepsilon_x &= \frac{\partial u}{\partial x} \\
\varepsilon_y &= \frac{\partial v}{\partial y} \\
\varepsilon_{xy} &= \frac{1}{2}\left(\frac{\partial u}{\partial y} + \frac{\partial v}{\partial x}\right) \\
\varepsilon_\theta &= \begin{cases} 0, & \text{plane strain} \\ \dfrac{u}{x}, & \text{axisymmetric} \end{cases}
\end{aligned} \tag{7}$$

Referring to Fig. 1, the strains in the cell bounded by the i-1, i, j-1, and j-lines are given by[2,4]

$$\begin{aligned}
\varepsilon_x &= \frac{1}{2Dx_i}\left(u_{i,j} + u_{i,j-1} - u_{i-1,j} - u_{i-1,j-1}\right) \\
\varepsilon_y &= \frac{1}{2Dy_j}\left(v_{i,j} + v_{i-1,j} - v_{i,j-1} - v_{i-1,j-1}\right) \\
\varepsilon_{xy} &= \frac{1}{4}\left[\frac{1}{Dx_i}\left(v_{i,j-1} + v_{i,j} - v_{i-1,j} - v_{i-1,j-1}\right)\right. \\
&\quad \left. + \frac{1}{Dy_j}\left(u_{i,j-1} + u_{i-1,j-1} - u_{i,j} - u_{i-1,j}\right)\right]
\end{aligned} \tag{8}$$

$$\Delta y_1 = \Delta y_2 = Dy_{j+1}$$

$$\Delta y_3 = \Delta y_4 = Dy_j .$$

For axisymmetric problems the $\sigma_{mn}/\rho x$ terms appearing in Eq. (1) are represented by:

$$\left(\frac{A}{\rho x}\right)_{i,j} = \frac{1}{M} \sum_{k=1}^{4} \frac{A_k}{\rho_k \bar{x}_k} , \qquad (5)$$

where M represents the number of cells surrounding the (i,j) node and $\bar{x}_k$ are defined as

$$\bar{x}_1 = \bar{x}_4 = x_{i+1/2}$$

$$\bar{x}_2 = \bar{x}_3 = x_{i-1/2} .$$

Equations (3) through (5) are also applicable for the case when (i,j) is not an interior node. To illustrate this point, the case when the j-line represents a surface in space where a stress boundary condition is applied will be discussed. Assuming material exists above the j-line, cells 3 and 4 do not exist for this case. Thus the summations of Eqs. (4) and (5) include $k = 1$ and $k = 2$ only. If the applied pressure is $P(x)$ and the applied shear stress is $\tau(x)$ Eq. (3) is evaluated using

$$\sigma_{x_3} = \sigma_{x_4} = 0$$

$$\sigma_{y_3} = -P\ (x_{i-1/2})$$

$$\sigma_{y_4} = -P\ (x_{i+1/2})$$

$$\sigma_{xy_3} = \tau\ (x_{i-1/2})$$

$$\sigma_{xy_4} = \tau\ (x_{i+1/2}) .$$

Finite differencing of the stress-displacement relationship completes the formulation. From Hooke's law, stresses and strains

and, for axisymmetric geometry, $\bar{\varepsilon}_\theta$ is calculated using

$$\varepsilon_\theta = \frac{\Delta v}{v_0} - \varepsilon_x - \varepsilon_\theta \tag{9}$$

where the bulk strain $\Delta v/v_0$ is evaluated using the following expressions:

$$\frac{\Delta v}{v_0} = \frac{\frac{1}{3} T_1 T_2 + \left(x_i - \frac{2}{3} Dx_i\right) T_3 + \left(x_i - \frac{1}{3} Dx_i\right) T_4}{2 T_1 x_{i-1/2}}$$

where

$$T_1 = Dx_i Dy_j$$

$$T_2 = 2u_{i,j-1} + 2u_{i-1,j} + u_{i,j} + u_{i-1,j-1}$$

$$T_3 = Dy_j \left(u_{i,j-1} - u_{i-1,j-1}\right) + Dx_i \left(v_{i-1,j} - v_{i-1,j-1}\right)$$

$$T_4 = Dy_j \left(u_{i,j} - u_{i-1,j}\right) + Dx_i \left(v_{i,j} - v_{i,j-1}\right)$$

Equations (2), (3), (4), (5), (8), and (9) represent the finite difference analog of Eqs. (1), (6), and (7).

APPENDIX E

If u, v and w are the x, y and z components of displacement, then the conservation of linear momentum may be written

$$\ddot{u} = \frac{\partial(P + \sigma_x)}{\rho\partial x} + \frac{\partial\sigma_{xy}}{\rho\partial y} + \frac{\partial\sigma_{xz}}{\rho\partial z} \tag{1}$$

$$\ddot{v} = \frac{\partial\sigma_{xy}}{\rho\partial x} + \frac{\partial(P + \sigma_x)}{\rho\partial y} + \frac{\partial\sigma_{yz}}{\rho\partial z} \tag{2}$$

$$\ddot{w} = \frac{\partial\sigma_{xz}}{\rho\partial x} + \frac{\partial\sigma_{yz}}{\rho\partial y} + \frac{\partial(P - \sigma_x - \sigma_y)}{\rho\partial z} \tag{3}$$

There will be eight elements surrounding a typical interior nodal point. These elements are labeled A through H as shown in Fig. 1. The exterior points of element A are labeled 1 through 8 as shown in Fig. 2.

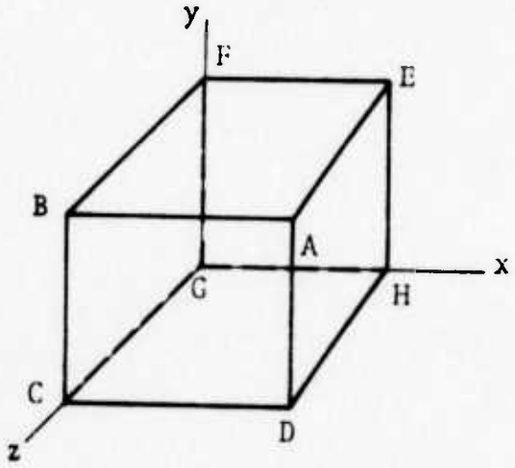

Figure 1.
Interior points of 8 elements are labeled A, B, C, D, E, F. G.

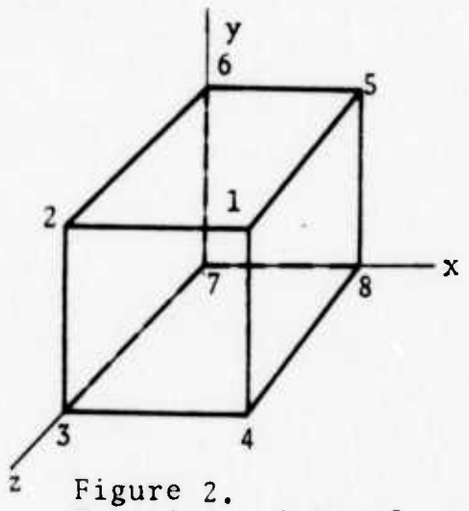

Figure 2.
Exterior points of zone A are labeled 1, 2, 3, 4, 5, 6, 7, 8.

The following calculations are performed for zone A.

$$\left(\frac{\partial u}{\partial x}\right)_A = \frac{u_{12} + u_{43} + u_{56} + u_{87}}{\Delta x+} \tag{4}$$

$$\left(\frac{\partial v}{\partial y}\right)_A = \frac{v_{14} + v_{23} + v_{67} + v_{58}}{\Delta y+} \tag{5}$$

$$\left(\frac{\partial w}{\partial z}\right)_A = \frac{w_{15} + w_{26} + w_{37} + w_{48}}{\Delta z+} \tag{6}$$

$$P_A = \frac{k}{8}\left[\left(\frac{\partial u}{\partial x}\right)_A + \left(\frac{\partial v}{\partial y}\right)_A + \left(\frac{\partial w}{\partial z}\right)_A\right] \tag{7}$$

$$(\sigma_x)_A = \frac{\mu}{12}\left[2\left(\frac{\partial u}{\partial x}\right)_A - \left(\frac{\partial v}{\partial y}\right)_A - \left(\frac{\partial w}{\partial z}\right)_A\right] \tag{8}$$

$$(\sigma_y)_A = \frac{\mu}{12}\left[2\left(\frac{\partial v}{\partial y}\right)_A - \left(\frac{\partial u}{\partial x}\right)_A - \left(\frac{\partial w}{\partial z}\right)_A\right] \tag{9}$$

$$(\sigma_{xy})_A = \frac{\mu}{8}\left[\frac{u_{14} + u_{23} + u_{67} + u_{58}}{\Delta y+} + \frac{\sigma_{12} + \sigma_{43} + \sigma_{56} + \sigma_{87}}{\Delta x+}\right] \tag{10}$$

$$(\sigma_{xz})_A = \frac{\mu}{8}\left[\frac{u_{15} + u_{26} + u_{37} + u_{48}}{\Delta z+} + \frac{w_{12} + w_{43} + w_{56} + w_{87}}{\Delta x+}\right] \tag{11}$$

$$(\sigma_{yz})_A = \frac{\mu}{8}\left[\frac{v_{15} + v_{26} + v_{37} + v_{48}}{\Delta z+} + \frac{w_{14} + w_{23} + w_{67} + w_{58}}{\Delta y+}\right] \tag{12}$$

where the following notation has been adopted

$$u_{12} = u_1 - u_2 \qquad v_{12} = v_1 - v_2, \text{ etc.}$$

$$\Delta x+ = \frac{x_8 - x_7}{2}, \quad \Delta y+ = \frac{y_6 - y_7}{2}, \quad \Delta z+ = \frac{z_3 - z_7}{2}$$

If Σ is a typical stress component ($P + \sigma_x$, $P + \sigma_y$, $P - \sigma_x - \sigma_y$, σ_{xy}, σ_{xz}, σ_{yz}) in Eqs. 1, 2 or 3, then the differenced form of a typical derivative term becomes

$$\frac{\partial \Sigma}{\rho \partial x} = \frac{\Sigma_{AB}(1 - \varepsilon^y)(1 - \varepsilon^z)}{\rho_A \Delta x^+ + \rho_B \Delta x^-} + \frac{\Sigma_{DC}\varepsilon^y(1 - \varepsilon^z)}{\rho_D \Delta x^+ + \rho_C \Delta x^-}$$

$$+ \frac{\Sigma_{EF}(1 - \varepsilon^y)\varepsilon^z}{\rho_E \Delta x^+ + \rho_F \Delta x^-} + \frac{\Sigma_{HG}\,\varepsilon^y\,\varepsilon^z}{\rho_H \Delta x^+ + \rho_G \Delta x^-} \tag{13}$$

$$\frac{\partial \Sigma}{\rho \partial y} = \frac{\Sigma_{AD}(1 - \varepsilon^x)(1 - \varepsilon^z)}{\rho_A \Delta y^+ + \rho_D \Delta y^-} + \frac{\Sigma_{BC}\varepsilon^x(1 - \varepsilon^z)}{\rho_B \Delta y^+ + \rho_C \Delta y^-}$$

$$+ \frac{\Sigma_{EH}(1 - \varepsilon^x)\varepsilon^z}{\rho_E \Delta y^+ + \rho_H \Delta y^-} + \frac{\Sigma_{FG}\,\varepsilon^x\,\varepsilon^z}{\rho_F \Delta y^+ + \rho_G \Delta y^-} \tag{14}$$

$$\frac{\partial \Sigma}{\rho \partial z} = \frac{\Sigma_{AE}(1 - \varepsilon^x)(1 - \varepsilon^y)}{\rho_A \Delta z^+ + \rho_E \Delta z^-} + \frac{\Sigma_{DH}\varepsilon y(1 - \varepsilon^x)}{\rho_D \Delta z^+ + \rho_H \Delta z^-}$$

$$+ \frac{\Sigma_{BF}\varepsilon^x(1 - \varepsilon^y)}{\rho_B \Delta z^+ + \rho_E \Delta z^-} + \frac{\Sigma_{CG}\,\varepsilon^x\,\varepsilon^y}{\rho_C \Delta z^+ + \rho_G \Delta z^-} \tag{15}$$

where

$$\varepsilon^x = \frac{\Delta x^+}{\Delta x^+ + \Delta x^-}\,, \quad \varepsilon^y = \frac{\Delta y^+}{\Delta y^+ + \Delta y^-}\,, \quad \varepsilon^z = \frac{\Delta z^+}{\Delta z^+ + \Delta z^-}$$

Equations 7 through 15 represent finite different approximations to Hooke's law and the conservation of linear momentum. In order to write the equations in this form, small displacement and elastic material behavior assumptions

required. Nonlinear material behavior will be simulated in the fault zone by recasting Eqs. 7 through 12 into a stress rate-strain rate formulation. This will entail saving six new (stress) variables at each grid location lying within the fault zone.